GOAL-ORIENTED ADAPTIVITY IN POINTWISE STATE CONSTRAINED OPTIMAL CONTROL OF PARTIAL DIFFERENTIAL EQUATIONS*

MICHAEL HINTERMÜLLER† AND RONALD H. W. HOPPE‡

Abstract. We derive primal-dual weighted goal-oriented a posteriori error estimates for pointwise state constrained optimal control problems for second order elliptic partial differential equations. The constraints give rise to a primal-dual weighted error term representing the mismatch in the complementarity system due to discretization. In the case of sufficiently regular active (or coincidence) sets and problem data, a further decomposition of the multiplier into a regular L^2-part on the active set and a singular part concentrated on the boundary between the active and inactive set allows us to further characterize the mismatch error. The paper ends with a report on the behavior of the error estimates for test cases including the case of singular active sets consisting of only smooth curves or points.

Key words. adaptive finite element method, a posteriori error estimate, pointwise state constraints, goal-oriented adaptivity, PDE-constrained optimization

AMS subject classifications. 49K20, 65K10, 65N30, 65N50

DOI. 10.1137/090761823

1. Introduction. This paper is devoted to mesh adaptivity for pointwise state constrained optimal control problems for elliptic partial differential equations (PDEs). A particular unilaterally constrained model problem is given by

$$\text{(P)} \qquad \begin{cases} \text{minimize} & J(y,u) \quad \text{over } (y,u) \in H_0^1(\Omega) \times L^2(\Omega), \\ \text{subject to} & -\Delta y = u + f \quad \text{in } \Omega, \\ & y \le b \quad \text{almost everywhere (a.e.) in } \Omega, \end{cases}$$

where $\Omega \subset \mathbb{R}^n$, $n \in \{2,3\}$, denotes some bounded domain with sufficiently smooth boundary $\Gamma = \partial\Omega$. Further, $f \in L^2(\Omega)$ and

$$b \in W^{1,r}(\Omega),\ r > n, \quad \text{with} \quad b|_\Gamma > 0, \tag{1.1}$$

represent given data. A typical choice for $J : H_0^1(\Omega) \times L^2(\Omega) \to \mathbb{R}$ is given by the tracking-type objective functional

$$J(y,u) = \frac{1}{2}\|y - z\|_{0,\Omega}^2 + \frac{\alpha}{2}\|u\|_{0,\Omega}^2,$$

where $z \in L^2(\Omega), \alpha > 0$ are given and $\|\cdot\|_{0,\Omega}$ denotes the usual norm in $L^2(\Omega)$. Further, we define $V^r := W_0^{1,r}(\Omega)$ for some $r > n$. Of course, more general objectives, other types of boundary conditions, and nonlinear governing equations are conceivable.

*Received by the editors June 11, 2009; accepted for publication (in revised form) July 31, 2010; published electronically November 16, 2010.

http://www.siam.org/journals/sicon/48-8/76182.html

†Institute of Mathematics, Humboldt University, Unter den Linden 6, D-10099 Berlin, Germany (hint@mathematik.hu-berlin.de), and Department of Mathematics and Scientific Computing, University of Graz, Heinrichstraße 36, A-8010 Graz, Austria (michael.hintermueller@uni-graz.at). This author's work was supported by the DFG Research Center MATHEON and by the Austrian Science Fund FWF under START-program Y305 "Interfaces and Free Boundaries."

‡Department of Mathematics, University of Houston, Houston, TX 77204-3008 (rohop@math.uh.edu), and Institute of Mathematics, University of Augsburg, D-86159 Augsburg, Germany (hoppe@math.uni-augsburg.de). This author's work was supported by the NSF under grants DMS-0707602, DMS-0810156, and DMS-0811153.

It is well known [7] that (P) admits a unique solution $(y^*, u^*) \in V^r \times L^2(\Omega)$ which is characterized by the following first order necessary (and in case of (P) also sufficient) optimality system written in weak form:

$$(\nabla y^*, \nabla v)_{0,\Omega} - (u^*, v)_{0,\Omega} = (f, v)_{0,\Omega} \quad \forall v \in H_0^1(\Omega), \tag{1.2a}$$

$$(\nabla p^*, \nabla w)_{0,\Omega} + \langle \lambda^*, w\rangle + (y, w)_{0,\Omega} = (z, w)_{0,\Omega} \quad \forall w \in V^r, \tag{1.2b}$$

$$\alpha u^* - p^* = 0, \tag{1.2c}$$

$$\langle \lambda^*, w - y^*\rangle \le 0 \quad \forall w \in V^r \text{ with } w \le b \text{ a.e. in } \Omega, \quad y^* \le b \text{ a.e. in } \Omega, \tag{1.2d}$$

where $p^* \in V^s$, with $V^s = \{w \in W^{1,s}(\Omega) : w|_\Gamma = 0\}$ and $r^{-1} + s^{-1} = 1$, and $\lambda^* \in M(\bar\Omega)$, with $M(\bar\Omega)$ denoting the set of regular Borel measures in $\bar\Omega$ and $\langle\cdot,\cdot\rangle$ the duality pairing between $M(\bar\Omega)$ and $C(\bar\Omega)$. Note that the latter pairing is realized as

$$\langle \lambda, w\rangle = \int_{\bar\Omega} w \, d\lambda$$

for $\lambda \in M(\bar\Omega)$ and $w \in V^r$. We point out that (1.2d) yields the so-called *complementarity system*

$$\lambda^* \ge 0, \quad y^* \le b \text{ a.e. in } \Omega, \quad \langle \lambda^*, y^* - b\rangle = 0. \tag{1.3}$$

The main difficulty in the numerical treatment of (P) is related to the measure-valuedness of the Lagrange multiplier λ^*. This affects the development of efficient solution procedures as well as the derivation of error estimates and mesh adaptation techniques. Concerning the development of efficient solution algorithms we mention the recent contributions [15, 20] as well as the survey [16] and the many references therein. In [8] the convergence of a finite element discretization of (P) is established. Recently, in [17, 18], residual-based a posteriori error estimates for an adaptive mesh refinement in the numerical solution of (P) were derived.

Besides adaptivity guided by residual-based a posteriori error estimates in the numerical solution process, frequently one is interested in achieving accuracy with respect to a prespecified target quantity or goal. This notion leads to so-called goal-oriented adaptivity, which was pioneered in [3] for unconstrained optimal control problems. For an excellent overview of this technique we refer the reader to [1, 2] and to [10] for a related technique. In [12, 23] this concept was further developed for pointwise control constrained optimal control problems, and in [4, 11, 24] it was applied to the state constrained case. When compared to residual-based estimators, it turns out that a primal-dual weighted goal-oriented approach with the objective function as the goal allows for coarser meshes while resolving the target quantity with the same accuracy. In contrast to the unconstrained case, the inequality constraints give rise to a so-called primal-dual weighted mismatch, which accounts for the error when discretizing the complementarity system (related to (1.3)). This error needs to be analyzed carefully in order to avoid overestimation which would result in estimates similar to the residual-based a posteriori estimates in [14] for a class of control constrained optimal control problems.

In the present paper we study the primal-dual weighted goal-oriented approach for pointwise state constrained problems of the type (P). In contrast to the work in [12] and the aforementioned papers on state constraints, the numerical realization of the inequalities and the discretization of the Lagrange multiplier are major issues. Based on a regularity assumption on the problem data and the active or coincidence

set with respect to the inequality constraint [6], we utilize a decomposition of the multiplier into a regular L^2-part and a singular part concentrated on the boundary of the active set. This allows us to further analyze the error due to the discretization of the complementarity system (1.3). In addition, we also address the singular case where the active set consists only of a lower dimensional manifold within the domain.

The rest of the paper is organized as follows. In section 2 we derive a primal-dual weighted error representation for the objective functional. It turns out that this representation is not fully a posteriori. Hence, in section 3 we establish an a posteriori error estimate up to the primal-dual mismatch in complementarity (cf. (2.21) in section 2). Depending on the regularity of the data and, more importantly, the coincidence or active set at the continuous solution, our analysis considers two distinct cases. In the regular case, the Lagrange multiplier pertinent to the pointwise state constraint can be decomposed into a regular L^2-part and a singular part concentrated on the boundary between the active set and its complement in Ω. In this situation we are able to further specialize the error representation. The paper ends by a report on numerical tests including the case of singular active sets.

Notation. Throughout we use $\|\cdot\|_{0,\Omega}$ and $(\cdot,\cdot)_{0,\Omega}$ for the usual $L^2(\Omega)$-norm and $L^2(\Omega)$-inner product, respectively. For convenience, with respect to the notation we shall not distinguish between the norm (respectively, inner product) for scalar-valued or vector-valued arguments. We also use $(\cdot,\cdot)_{0,\mathcal{S}}$, which is the $L^2(\mathcal{S})$-inner product over a (measurable) subset $\mathcal{S} \subset \Omega$. By $|\cdot|_{1,\Omega}$ we denote the $H^1(\Omega)$-seminorm $|y|_{1,\Omega} = \|\nabla y\|_{0,\Omega}$, which, by the Poincaré–Friedrichs inequality, is a norm on $H_0^1(\Omega)$. The norm in $H^1(\Omega)$ is written as $\|\cdot\|_{1,\Omega}$. By $\mathcal{T}_h = \mathcal{T}_h(\Omega)$ we denote a shape regular finite element triangulation of the domain Ω. The subscript $h = \max\{\operatorname{diam}(T) | T \in \mathcal{T}_h\}$ indicates the mesh size of $\mathcal{T}_h$. The vertices or nodes of the mesh are given by $\mathbf{x}_j$, $j = 1, \ldots, N_h$. The sets of vertices and edges in $S \subset \Omega$ are denoted by $\mathcal{N}_h(S)$ and $\mathcal{E}_h(S)$, respectively. Finally, the notation $a \lesssim b$ implies that there exists a constant $C > 0$ (depending only on the shape regularity of the finite element triangulation) such that $a \leq C\, b$.

2. Primal-dual weighted error representation. For deriving the structure of the new error estimate which takes into account the pointwise inequality constraints, we focus on our model problem (P). Its corresponding first order optimality characterization (1.2) can be derived from the pertinent Lagrange function $\mathcal{L} : V^r \times V^s \times L^2(\Omega) \times M(\bar{\Omega}) \to \mathbb{R}$ with

$$\mathcal{L}(y, p, u, \lambda) = J(y, u) + (\nabla y, \nabla p)_{0,\Omega} - (u + f, p)_{0,\Omega} + \langle \lambda, y - b \rangle. \tag{2.1}$$

For convenience we use $x := (y, p, u)$, $x^* = (y^*, p^*, u^*)$, and $X = V^r \times V^s \times L^2(\Omega)$. Obviously, system (1.2a)–(1.2c) is equivalent to

$$\nabla_x \mathcal{L}(x^*, \lambda^*)(\delta x) = 0 \quad \forall \delta x \in X. \tag{2.2}$$

Here we consider the following finite element discretization of the problem of interest: We assume that the domain is polyhedral such that the boundary is exactly represented by boundaries of triangles T. By V_h we denote the space of continuous piecewise linear finite elements over $\bar{\Omega}$. The discrete space X_h is given by

$$X_h = V_h \times V_h \times V_h.$$

Here we use the fact that $\alpha u^* = p^*$, which implies that u^* inherits the V^s-regularity of p^*. Therefore, both quantities are discretized using the same ansatz.

For obtaining a discrete version of (1.2) we have to clarify how the discrete inequality constraint on the state is realized and, in connection with this choice, how the Lagrange multiplier is discretized. In fact, the discrete constraints read

$$y_h(a) \le b(a) \quad \forall a \in \mathcal{N}_h(\Omega). \tag{2.3}$$

As a consequence, the discrete multiplier pertinent to (2.3) is represented by

$$\lambda_h = \sum_{a \in \mathcal{N}_h(\Omega)} \kappa_a \delta_a, \tag{2.4}$$

where δ_a denotes the Dirac measure concentrated in $a \in \mathcal{N}_h(\Omega)$. Subsequently we use

$$M_h = \left\{ \lambda_h = \sum_{a \in \mathcal{N}_h(\Omega)} \kappa_a \delta_a : \ \kappa_a \in \mathbb{R} \ , \ a \in \mathcal{N}_h(\Omega) \right\}.$$

In order to obtain a full complementarity system (compare (1.2d)) we define I_h as the Lagrange interpolation operator associated with the nodes $a \in \mathcal{N}_h(\Omega)$, and we set

$$b_h = I_h b.$$

Moreover, f_h and z_h are chosen as the L^2-projections of f and z onto V_h. Now the discrete version of (1.2) is given by

$$(\nabla y_h^*, \nabla v_h)_{0,\Omega} - (u_h^*, v_h)_{0,\Omega} = (f_h, v_h)_{0,\Omega} \quad \forall v_h \in V_h, \tag{2.5a}$$

$$(\nabla p_h^*, \nabla w_h)_{0,\Omega} + \langle \lambda_h^*, w_h \rangle + (y_h, w_h)_{0,\Omega} = (z_h, w_h)_{0,\Omega} \quad \forall w_h \in V_h, \tag{2.5b}$$

$$\alpha u_h^* - p_h^* = 0, \tag{2.5c}$$

$$y_h^*(a) \le b_h(a), \quad \kappa_a^* \ge 0, \quad \forall a \in \mathcal{N}_h(\Omega), \quad \langle \lambda_h^*, y_h^* - b_h \rangle = 0. \tag{2.5d}$$

It is straightforward that (2.5) is the first order necessary and sufficient condition of the discrete version of (P) given by

$$(\mathrm{P}_h) \qquad \begin{cases} \text{minimize} & J_h(y_h, u_h) \quad \text{over } (y_h, u_h) \in V_h \times V_h, \\ \text{subject to} & (\nabla y_h, \nabla v_h)_{0,\Omega} = (u_h + f_h, v_h)_{0,\Omega} \quad \forall v_h \in V_h, \\ & y_h(a) \le b_h(a) \quad \forall a \in \mathcal{N}_h(\Omega), \end{cases}$$

where $J_h(y_h, u_h) = \frac{1}{2}\|y_h - z_h\|_{0,\Omega}^2 + \frac{\alpha}{2}\|u_h\|_{0,\Omega}^2$. The discrete Lagrangian is given by

$$\begin{aligned} \mathcal{L}_h(x_h, \lambda_h) = J_h(y_h, u_h) + (\nabla y_h, \nabla p_h)_{0,\Omega} - (u_h + f_h, p_h)_{0,\Omega} \\ + \langle \lambda_h, y_h - b_h \rangle. \end{aligned} \tag{2.6}$$

Similar to the continuous case, (2.5a)–(2.5c) is given by

$$\nabla_x \mathcal{L}_h(x_h^*, \lambda_h^*)(\delta x_h) = 0 \quad \forall \delta x_h \in X_h. \tag{2.7}$$

Note that for $x \in X$, $\lambda \in \mathcal{M}(\bar{\Omega})$ and $x_h \in X_h$, $\lambda_h \in \mathcal{M}_h$ we obtain the relations

$$\mathcal{L}(x, \lambda_h) = \mathcal{L}(x, \lambda) + \langle \lambda_h - \lambda, y - b \rangle, \tag{2.8}$$

$$\nabla_x \mathcal{L}(x_h, \lambda_h)(\delta x_h) = \nabla_x \mathcal{L}(x_h, \lambda)(\delta x_h) + \langle \lambda_h - \lambda, \delta y_h \rangle \tag{2.9}$$

for all $\delta x_h = (\delta y_h, \delta p_h, \delta u_h) \in X_h$. Here we use $V^r \subset \mathcal{C}(\bar{\Omega})$ by the Sobolev embedding theorem. Moreover, for our model problem (P) the second derivative of $\mathcal{L}$ with respect to x does not depend on x and λ. Thus, we can write $\nabla_{xx}\mathcal{L}(\delta x, \widehat{\delta x})$ instead of $\nabla_{xx}\mathcal{L}(x,\lambda)(\delta x, \widehat{\delta x})$. Similar observations hold true for $\mathcal{L}_h$. Due to $X_h \subset X$, we have for $\delta x_h = (\delta y_h, \delta p_h, \delta u_h) \in X_h$

$$
\begin{aligned}
0 &= \nabla_x \mathcal{L}(x^*, \lambda^*)(\delta x_h) \\
&= \nabla_x \mathcal{L}(x_h^*, \lambda^*)(\delta x_h) + \nabla_{xx}\mathcal{L}(x^* - x_h^*, \delta x_h) \\
&= \nabla_x \mathcal{L}(x_h^*, \lambda_h^*)(\delta x_h) + \langle \lambda^* - \lambda_h^*, \delta y_h\rangle + \nabla_{xx}\mathcal{L}(x^* - x_h^*, \delta x_h) \\
&= \nabla_x \mathcal{L}_h(x_h^*, \lambda_h^*)(\delta x_h) - (f - f_h, \delta p_h)_{0,\Omega} - (z - z_h, \delta y_h)_{0,\Omega} \\
&\quad + \langle \lambda^* - \lambda_h^*, \delta y_h\rangle + \nabla_{xx}\mathcal{L}(x^* - x_h^*, \delta x_h) \\
&= \langle \lambda^* - \lambda_h^*, \delta y_h\rangle + \nabla_{xx}\mathcal{L}(x^* - x_h^*, \delta x_h) - (f - f_h, \delta p_h)_{0,\Omega} \\
&\quad - (z - z_h, \delta y_h)_{0,\Omega}.
\end{aligned} \tag{2.10}
$$

Since (2.9) and the first two lines in (2.10) obviously hold true for δx_h replaced by any element in X, from this we further derive the relations

$$
\begin{aligned}
&\nabla_{xx}\mathcal{L}(x_h^* - x^*, x_h^* - x^*) \\
&\qquad = \nabla_{xx}\mathcal{L}(x_h^* - x^*, x_h^* - x^* + \delta x_h) - \langle \lambda^* - \lambda_h^*, \delta y_h\rangle \\
&\qquad\quad + (f - f_h, \delta p_h)_{0,\Omega} + (z - z_h, \delta y_h)_{0,\Omega},
\end{aligned} \tag{2.11}
$$

$$
\nabla_x \mathcal{L}(x_h^*, \lambda^*)(x^* - x_h^* - \delta x_h) = \nabla_{xx}\mathcal{L}(x_h^* - x^*, x^* - x_h^* - \delta x_h), \tag{2.12}
$$

and also

$$
\begin{aligned}
&\nabla_x \mathcal{L}(x_h^*, \lambda_h^*)(x^* - x_h^* - \delta x_h) \\
&\qquad = \langle \lambda_h^* - \lambda^*, y^* - y_h^* - \delta y_h\rangle + \nabla_{xx}\mathcal{L}(x_h^* - x^*, x^* - x_h^* - \delta x_h).
\end{aligned} \tag{2.13}
$$

Next we establish a representation of the difference of the continuous and discrete goal in terms of the Hessian of the Lagrangian and additional contributions.

THEOREM 2.1. *Let $(x^*, \lambda^*) \in X \times M(\bar{\Omega})$ and $(x_h^*, \lambda_h^*) \in X_h \times M_h$ denote the solution of* (1.2) *and its finite dimensional counterpart* (2.5). *Then*

$$
\begin{aligned}
J(y^*, u^*) - J_h(y_h^*, u_h^*) = &-\frac{1}{2}\nabla_{xx}\mathcal{L}(x_h^* - x^*, x_h^* - x^*) \\
&+ \langle \lambda^*, y_h^* - b\rangle + \widehat{osc}_h^{(1)},
\end{aligned} \tag{2.14}
$$

where the data oscillations $\widehat{osc}_h^{(1)}$ are given by

$$
\begin{aligned}
\widehat{osc}_h^{(1)} &:= \sum_{T \in \mathcal{T}_h} \widehat{osc}_T^{(1)}\ , \\
\widehat{osc}_T^{(1)} &:= (y_h^* - z_h, z_h - z)_{0,T} + \frac{1}{2}\|z - z_h\|_{0,T}^2 + (f_h - f, p_h^*)_{0,T}.
\end{aligned} \tag{2.15}
$$

Proof. Observe that $J(y^*, u^*) = \mathcal{L}(x^*, \lambda^*)$ and $J_h(y_h^*, u_h^*) = \mathcal{L}_h(x_h^*, \lambda_h^*)$. Using

Taylor expansions and (2.8)–(2.9), we obtain

$$\begin{aligned}
J(y^*,u^*) - J_h(y_h^*,u_h^*) &= \mathcal{L}(x^*,\lambda^*) - \mathcal{L}_h(x_h^*,\lambda_h^*)\\
&= \mathcal{L}(x^*,\lambda^*) - \mathcal{L}_h(x^*,\lambda_h^*) - \nabla_x\mathcal{L}_h(x^*,\lambda_h^*)(x_h^*-x^*)\\
&\quad - \frac{1}{2}\nabla_{xx}\mathcal{L}_h(x_h^*-x^*,x_h^*-x^*)\\
&= J(y^*,u^*) - J_h(y^*,u^*) + (f_h-f,p^*)_{0,\Omega} - \langle\lambda_h^*,y^*-b_h\rangle\\
&\quad - \nabla_x\mathcal{L}_h(x^*,\lambda_h^*)(x_h^*-x^*) - \frac{1}{2}\nabla_{xx}\mathcal{L}_h(x_h^*-x^*,x_h^*-x^*)\\
&= \widehat{osc}_h^{(1)} - \langle\lambda_h^*,y^*-b_h\rangle - \nabla_x\mathcal{L}(x^*,\lambda_h^*)(x_h^*-x^*)\\
&\quad - \frac{1}{2}\nabla_{xx}\mathcal{L}_h(x_h^*-x^*,x_h^*-x^*)\\
&= \widehat{osc}_h^{(1)} - \langle\lambda_h^*,y^*-y_h^*\rangle + \langle\lambda^*-\lambda_h^*,y_h^*-y^*\rangle\\
&\quad - \frac{1}{2}\nabla_{xx}\mathcal{L}_h(x_h^*-x^*,x_h^*-x^*)\\
&= \widehat{osc}_h^{(1)} + \langle\lambda^*,y_h^*-b\rangle - \frac{1}{2}\nabla_{xx}\mathcal{L}_h(x_h^*-x^*,x_h^*-x^*),
\end{aligned}$$

where we also used the complementarity relations (1.2d) and (2.5d) as well as (2.2) and (2.7). ∎

Remark 2.1. In the case where $\lambda^*=0$ and $\lambda_h^*=0$ one readily finds

$$\begin{aligned}
J(y^*,u^*) - J_h(y_h^*,u_h^*) &= \frac{1}{2}\nabla_x\mathcal{L}_h(x_h^*,\lambda_h^*)(x^*-x_h^*-\delta x_h)\\
&\quad + \frac{1}{2}(f_h-f,p^*-p_h^*)_{0,\Omega} + \frac{1}{2}(z_h-z,y^*-y_h^*)_{0,\Omega}\\
&\quad + \widehat{osc}_h^{(1)},
\end{aligned}$$

which corresponds to the result in [3, Proposition 4.1] for the unconstrained version of (P).

Remark 2.2. The contribution $\langle\lambda^*,y_h^*-b\rangle$ due to the pointwise inequality constraints can be rewritten as

$$\langle\lambda^*,y_h^*-b\rangle = \langle\lambda^*,y_h^*-b_h\rangle + \langle\lambda^*,b_h-b\rangle. \tag{2.16}$$

Observe that (2.16) reflects the *error in complementarity*. In fact, the second term represents the data oscillation in the upper bound on the state weighted by the continuous Lagrange multiplier, whereas the first term on the right-hand side of (2.16) captures the *mismatch in complementarity*.

We now introduce interpolation operators

$$i_h^y : V^{\bar r} \to V_h,\ r>\bar r>n, \qquad i_h^p : V^{\bar s} \to V_h\ ,\ 1<s<\bar s<\frac{n}{n-1}, \tag{2.17}$$

such that for all $y\in V^r$ and $p\in V^s$

$$\left(h_T^{r(t-1)}\|i_h^y y - y\|_{t,r,T}^r\right)^{1/r} \lesssim \|y\|_{1,r,D_T}, \quad 0\le t\le 1, \tag{2.18a}$$

$$\left(h_T^{-r}\|i_h^y y - y\|_{0,r,T}^r + h_T^{-r/2}\|i_h^y y - y\|_{0,r,\partial T}^r\right)^{1/r} \lesssim \|y\|_{1,r,D_T}, \tag{2.18b}$$

$$\left(h_T^{-s}\|i_h^p p - p\|_{0,s,T}^s + h_T^{-s/2}\|i_h^p p - p\|_{0,s,\partial T}^s\right)^{1/s} \lesssim \|p\|_{1,s,D_T}, \tag{2.18c}$$

where $D_T := \bigcup\{T' \in \mathcal{T}_h \mid \mathcal{N}_h(T') \cap \mathcal{N}_h(T) \neq \emptyset\}$.

Examples for interpolation operators satisfying (2.18a)–(2.18c) are the Scott–Zhang interpolation operators (cf., e.g., [22]). Now we can further dwell on the evaluation of the Hessian of the Lagrangian and represent the error by means of *primal-dual residuals*, the *primal-dual mismatch in complementarity*, and *oscillation terms*.

THEOREM 2.2. *Let the assumptions of Theorem* 2.1 *be satisfied, and let* i_h^w, $w \in \{y, p\}$, *be the interpolation operators* (2.17). *Then, the following holds:*

$$J(y^*, u^*) - J_h(y_h^*, u_h^*) = -r(i_h^w w^* - w^*) + \psi_h + \widehat{osc}_h. \tag{2.19}$$

Here, $r(i_h^w w^* - w^*)$ *stands for the primal-dual weighted residuals*

$$\begin{aligned} r(i_h^w w^* - w^*) := \frac{1}{2}\Big(& (y_h^* - z_h, i_h^y y^* - y^*)_{0,\Omega} + (\nabla(i_h^y y^* - y^*), \nabla p_h^*)_{0,\Omega} \\ & + (\nabla(i_h^p p^* - p^*), \nabla y_h^*)_{0,\Omega} - (u_h^* + f_h, i_h^p p^* - p^*)_{0,\Omega}\Big), \end{aligned} \tag{2.20}$$

the term ψ_h *represents the primal-dual mismatch in complementarity*

$$\psi_h := \frac{1}{2}\big(\langle \lambda^*, y_h^* - b\rangle + \langle \lambda_h^*, b_h - y^*\rangle\big), \tag{2.21}$$

and $\widehat{osc}_h$ *refers to the data oscillations*

$$\widehat{osc}_h := \widehat{osc}_h^{(1)} + \widehat{osc}_h^{(2)}, \tag{2.22}$$

where $\widehat{osc}_h^{(1)}$ *is given by* (2.15) *and* $\widehat{osc}_h^{(2)}$ *by*

$$\widehat{osc}_h^{(2)} := \frac{1}{2}\sum_{T\in\mathcal{T}_h}\Big((f - f_h, p_h^* - p^*)_{0,T} + (z - z_h, y_h^* - y^*)_{0,T}\Big). \tag{2.23}$$

Proof. Utilizing (2.11)–(2.12) and considering $\delta x_h = (\delta y_h, \delta p_h, \delta u_h) \in X_h$, we obtain

$$\begin{aligned} J(y^*, u^*) - J_h(y_h^*, u_h^*) &= \frac{1}{2}\nabla_{xx}\mathcal{L}(x, \lambda_h^*)(x^* - x_h^*, x_h^* - x^* + \delta x_h) \\ &\quad + \frac{1}{2}\langle \lambda^* - \lambda_h^*, \delta y_h\rangle + \frac{1}{2}(f_h - f, \delta p_h)_{0,\Omega} + \frac{1}{2}(z_h - z, \delta y_h)_{0,\Omega} \\ &\quad + \langle \lambda^*, y_h^* - b\rangle + \widehat{\mathrm{osc}}_h^{(1)} \\ &= -\frac{1}{2}\nabla_x\mathcal{L}(x_h^*, \lambda_h^*)(x_h^* - x^* + \delta x_h) + \frac{1}{2}\langle \lambda_h^* + \lambda^*, y_h^* - y^*\rangle \\ &\quad + \frac{1}{2}(f_h - f, \delta p_h)_{0,\Omega} + \frac{1}{2}(z_h - z, \delta y_h)_{0,\Omega} + \widehat{\mathrm{osc}}_h^{(1)} \\ &= -\frac{1}{2}\nabla_x\mathcal{L}_h(x_h^*, \lambda_h^*)(x_h^* - x^* + \delta x_h) + \frac{1}{2}\langle \lambda_h^* + \lambda^*, y_h^* - y^*\rangle \\ &\quad + \frac{1}{2}(f - f_h, p_h^* - p^*)_{0,\Omega} + \frac{1}{2}(z - z_h, y_h^* - y^*)_{0,\Omega} + \widehat{\mathrm{osc}}_h^{(1)}. \end{aligned}$$

Choosing $\delta x_h = (i_h^y y^* - y_h^*, i_h^p p^* - p_h^*, i_h^u u^* - u_h^*) \in X_h$ and using complementary slackness, we continue with

$$\begin{aligned} J(y^*, u^*) - J_h(y_h^*, u_h^*) = & -\frac{1}{2}\nabla_x\mathcal{L}_h(x_h^*, \lambda_h^*)(i_h x^* - x^*) + \frac{1}{2}\big[\langle \lambda_h^*, b_h - y^*\rangle + \langle \lambda^*, y_h^* - b\rangle\big] \\ & + \frac{1}{2}(f - f_h, p_h^* - p^*)_{0,\Omega} + \frac{1}{2}(z - z_h, y_h^* - y^*)_{0,\Omega} + \widehat{\mathrm{osc}}_h^{(1)}, \end{aligned}$$

where $i_h x^* := (i_h^y y^*, i_h^p p^*, i_h^u u^*)$. The assertion now follows from (2.1), $\langle \lambda_h^*, i_h^y y^* - y^* \rangle = 0$ due to $(i_h^y y^*)(a) = y^*(a)$ for $a \in \mathcal{N}_h(\mathcal{T}_h)$, and $\alpha u_h^* - p_h^* = 0$ a.e. in Ω. ∎

We remark that so far the only easily computable term on the right-hand side in (2.19) is the oscillation term $\widehat{osc}_h^{(1)}$. All other terms still involve the unknown optimal state y^*, the optimal adjoint state p^*, and/or the optimal multiplier λ^*. In the next section, we will deal with those remaining terms and provide approximations that are truly a posteriori in nature.

3. Primal-dual weighted a posteriori error estimate.

3.1. Primal-dual weighted residuals. First, we are concerned with an evaluation of the primal-dual weighted residuals.

THEOREM 3.1. *Under the assumptions of Theorem* 2.2 *it holds that*

$$|r(i_h^w w^* - w^*)| \lesssim \sum_{T \in \mathcal{T}_h} \left(\rho_T^{(1)} \omega_T^{(1)} + \rho_T^{(2)} \omega_T^{(2)} \right). \tag{3.1}$$

Here, for the residuals $\rho_T^{(i)}, 1 \le i \le 2$, *we have*

$$\rho_T^{(1)} := \left(\|r_T^{(1)}\|_{0,r,T}^r + h_T^{-r/2} \|r_{\partial T}^{(1)}\|_{0,r,\partial T}^r \right)^{1/r}, \tag{3.2a}$$

$$r_T^{(1)} := u_h^* + f_h, \qquad r_{\partial T}^{(1)} := \frac{1}{2} \nu_{\partial T} \cdot [\nabla y_h^*], \quad T \in \mathcal{T}_h,$$

$$\rho_T^{(2)} := \left(\|r_T^{(2)}\|_{0,s,T}^s + h_T^{-s/2} \|r_{\partial T}^{(2)}\|_{0,r,\partial T}^s \right)^{1/s}, \tag{3.2b}$$

$$r_T^{(2)} := y_h^* - z_h, \qquad r_{\partial T}^{(2)} := \frac{1}{2} \nu_{\partial T} \cdot [\nabla p_h^*], \quad T \in \mathcal{T}_h,$$

where $[\cdot]$ *denotes the jump across* ∂T. *The associated weights* $\omega_T^{(i)}, 1 \le i \le 2$, *are given by*

$$\omega_T^{(1)} := \left(\|i_h^p p^* - p^*\|_{0,s,T}^s + h_T^{s/2} \|i_h^p p^* - p^*\|_{0,s,\partial T}^s \right)^{1/s}, \tag{3.3a}$$

$$\omega_T^{(2)} := \left(\|i_h^y y^* - y^*\|_{0,r,T}^r + h_T^{r/2} \|i_h^y y^* - y^*\|_{0,r,\partial T}^r \right)^{1/r}. \tag{3.3b}$$

Proof. Applying Green's formula on each element, we obtain

$$\begin{aligned} 2r(i_h^w w^* - w^*) = &\sum_{T \in \mathcal{T}_h} [-(r_T^{(1)}, i_h^p p^* - p^*)_{0,T} + (r_{\partial T}^{(1)}, i_h^p p^* - p^*)_{0,\partial T}] \\ &+ \sum_{T \in \mathcal{T}_h} [(r_T^{(2)}, i_h^y y^* - y^*)_{0,T} + (r_{\partial T}^{(2)}, i_h^y y^* - y^*)_{0,\partial T}] \,. \end{aligned} \tag{3.4}$$

Denoting the two terms on the right-hand side in (3.4) by I_1 and I_2, respectively, by straightforward estimation for I_1 we find

$$\begin{aligned} |I_1| &\le \sum_{T\in\mathcal{T}_h} [|(r_T^{(1)}, i_h^p p^* - p^*)_{0,T}| \\ &\qquad + |(h_T^{-1/2} r_{\partial T}^{(1)}, h_T^{1/2}(i_h^p p^* - p^*))_{0,\partial T}|] \\ &\le \sum_{T\in\mathcal{T}_h} [\|r_T^{(1)}\|_{0,r,T} \|i_h^p p^* - p^*\|_{0,s,T} \\ &\qquad + h_T^{-1/2} \|r_{\partial T}^{(1)}\|_{0,r,\partial T} h_T^{1/2} \|i_h^p p^* - p^*\|_{0,s,\partial T}] \\ &\lesssim \sum_{T\in\mathcal{T}_h} \rho_T^{(1)} \omega_T^{(1)}. \end{aligned} \tag{3.5}$$

Likewise, for I_2 we obtain

$$|I_2| \lesssim \sum_{T\in\mathcal{T}_h} \rho_T^{(2)} \omega_T^{(2)}. \tag{3.6}$$

Summing up (3.5)–(3.6) gives the assertion. ∎

The weights $\omega_T^{(i)}, 1 \le i \le 2$, for the residuals $\rho_T^{(i)}$ still depend on the unknown optimal state $y^* \in V^r$ and optimal adjoint state $p^* \in V^s$. One way to overcome this difficulty is to replace $i_h^y y^* - y^*$ and $i_h^p p^* - p^*$ in (3.3a)–(3.3b) by $i_H^{(2)} y_h^* - y_h^*$ and $i_H^{(2)} p_h^* - p_h^*$, where $i_H^{(2)} y_h^*$ and $i_H^{(2)} p_h^*$ are the quadratic Lagrange interpolants of y_h^*, p_h^* on a coarser mesh $\mathcal{T}_H$ with $\mathcal{T}_h \subset \mathcal{T}_H$ using the corresponding nodal values of y_h^*, p_h^* (cf., e.g., [1, 11]). Here, we proceed in a slightly different way: We estimate $i_h^y y^* - y^*$ and $i_h^p p^* - p^*$ by (2.18a)–(2.18c) and replace $\|y^*\|_{1,r,D_T}, \|p^*\|_{1,s,D_T}$ by $\|y_h^*\|_{1,r,D_T}, \|p_h^*\|_{1,s,D_T}$. We thus obtain the computable approximations

$$\hat{\omega}_T^{(1)} := h_T \, \|p_h^*\|_{1,s,D_T}, \tag{3.7a}$$

$$\hat{\omega}_T^{(2)} := h_T \, \|y_h^*\|_{1,r,D_T}. \tag{3.7b}$$

Substituting $\omega_T^{(i)}$ by $\hat{\omega}_T^{(i)}, 1 \le i \le 2$, we obtain the *primal-dual weighted a posteriori error estimator*

$$\begin{aligned} \eta_h^{PD} &:= \sum_{T\in\mathcal{T}_h} \eta_T^{PD}, \\ \eta_T^{PD} &:= \sum_{i=1}^{2} \rho_T^{(i)} \hat{\omega}_T^{(i)}, \quad T \in \mathcal{T}_h. \end{aligned} \tag{3.8}$$

3.2. Primal-dual mismatch in complementarity. The term $\psi_h = \psi_h(y^*, y_h^*)$ as given by (2.21) is related to errors coming from complementary slackness. For its interpretation, we define the active set $\mathcal{A}^*$ and the inactive set $\mathcal{I}^*$ at the optimal solution (x^*, λ^*) of (P) by

$$\mathcal{A}^* := \{\mathbf{x} \in \Omega : y^*(\mathbf{x}) = b(\mathbf{x})\}, \quad \mathcal{I}^* := \Omega \setminus \mathcal{A}^*. \tag{3.9}$$

The discrete analogues of $\mathcal{A}^*$ and $\mathcal{I}^*$ are defined as follows: First, let

$$A_h^* := \{j \in \{1, \dots, N_h\} : y_h^*(\mathbf{x}_j) = b(\mathbf{x}_j)\}, \quad I_h^* := \{1, \dots, N_h\} \setminus \mathcal{A}_h^* \tag{3.10}$$

denote the active and inactive vertices, respectively. Then the discrete active and inactive sets are, respectively, defined by

$$\mathcal{A}_h^* := \{T \in \mathcal{T}_h(\Omega) : \mathcal{N}_h(T) \subset A_h^*\}, \quad \mathcal{I}_h^* := \mathcal{T}_h(\Omega) \setminus \mathcal{A}_h^*. \tag{3.11}$$

Next we define $J^* = \{j \in \{1, \dots, N_h\} : \mathbf{x}_j \in \mathcal{I}^*\}$. Then we have

$$\langle \lambda_h^*, b_h - y^* \rangle = \langle \lambda_h^*, b - y^* \rangle = \sum_{j \in J^*} \kappa_j^* \left(b(\mathbf{x}_j) - y^*(\mathbf{x}_j) \right) \geq 0$$

since $b_h(\mathbf{x}_j) = b(\mathbf{x}_j)$ for all $j = 1, \dots, N_h$. Here and below, we use κ_j^* instead of $\kappa_{\mathbf{x}_j}^*$ for $\mathbf{x}_j \in \mathcal{N}_h(\Omega)$. Hence, the right-hand side above represents the *primal-dual weighted mismatch in complementarity in* $\mathcal{I}^*$.

Due to the continuous and discrete complementarity systems (1.2d) and (2.5d), ψ_h is equivalent to

$$\psi_h = \frac{1}{2} \big[\langle \lambda_h^* - \lambda^*, b_h - y^* \rangle + \langle \lambda_h^* - \lambda^*, b - y_h^* \rangle + \langle \lambda_h^* + \lambda^*, b_h - b \rangle \big]. \tag{3.12}$$

Recall that $\langle \lambda_h^*, y_h^* - b \rangle = \langle \lambda_h^*, y_h^* - b_h \rangle = 0$ as well as $\langle \lambda_h^*, b - b_h \rangle = 0$ for any $\lambda_h \in \mathcal{M}_h$. These facts would allow us to simplify the above expression even further. For our subsequent treatment of the dual products on the right-hand side in (3.12), following [6], we will consider the so-called regular and nonregular cases with regard to a classification of the structure of the Lagrange multiplier associated with the state constrained optimal control problem.

3.2.1. Regular case. We assume that b in (P) is such that $\Delta b \in H^2(\Omega)$ and that the coincidence set $\mathcal{A}^*$ satisfies

$$\begin{cases} \mathcal{A}^* = \bigcup_{i=1}^m \mathcal{A}_i^*, \quad \mathrm{cl}(\mathrm{int}(\mathcal{A}_i^*)) = \mathcal{A}_i^*, \quad 1 \leq i \leq m, \\ \mathcal{A}_i^* \cap \mathcal{A}_j^* = \emptyset, \quad 1 \leq i \neq j \leq m, \\ \mathcal{A}_i^*, \ 1 \leq i \leq m, \ \text{is connected with the } C^{1,1}\text{-boundary.} \end{cases} \tag{A$_1$}$$

Since $\mathcal{A}^* \cap \Gamma = \emptyset$ is already implied by our assumption (1.1) on the data, i.e., a Slater condition for (P), in view of [6, Theorem 2] we have

$$p^* \in V^s, \quad p^*|_{\mathrm{int}(\mathcal{A}^*)} \in H^2(\mathrm{int}(\mathcal{A}^*)), \quad p^*|_{\mathcal{I}^*} \in H^2(\mathcal{I}^*). \tag{3.13}$$

Moreover, denoting by $\mathcal{F}^* := \mathcal{A}^* \cap \mathrm{cl}(\mathcal{I}^*)$ the free boundary between the coincidence set and the noncoincidence set, it holds that

$$p^* = -\alpha \, \Delta b \quad \text{in } \mathcal{A}^*, \tag{3.14a}$$

$$-\Delta p^* = z - y^* \quad \text{in } \mathcal{I}^*, \tag{3.14b}$$

$$p^* = -\alpha \, \Delta b \quad \text{on } \mathcal{F}^*,$$

$$\lambda^* = \mu^* + \mu_{\mathcal{F}^*}^*, \quad \mu^* \in L_+^2(\Omega) \ , \ \mu_{\mathcal{F}^*}^* \in H_+^{1/2}(\mathcal{F}^*), \tag{3.14c}$$

where

$$\mu^* = \begin{cases} 0 & \text{on } \mathcal{I}^*, \\ z - b - \alpha \, \Delta^2 b & \text{on } \mathcal{A}^*, \end{cases} \tag{3.15a}$$

$$\mu_{\mathcal{F}^*}^* = -\frac{\partial p^*|_{\mathcal{I}^*}}{\partial n_{\mathcal{I}^*}} + \alpha \frac{\partial \Delta b}{\partial n_{\mathcal{A}^*}}, \tag{3.15b}$$

and $L^2_+(\Omega)$ as well as $H^{1/2}_+(\mathcal{F}^*)$ denote the nonnegative cones in $L^2(\Omega)$ and $H^{1/2}(\mathcal{F}^*)$, respectively.

Following [13] (see also [14, 19]), we provide an approximation of the continuous coincidence set $\mathcal{A}^*$ by

$$\chi_h^{\mathcal{A}^*} := I - \frac{b - i_h^y y_h^*}{\gamma h^t + b - i_h^y y_h^*},$$

where $0 < \gamma \leq 1$ and $t > 0$ are fixed (e.g., $\gamma = 0.5$ and $t = 1.0$). Denoting by $\chi(S)$ the characteristic function of $S \subset \Omega$, for $T \subset \mathcal{A}^*$ we find

$$\|\chi(\mathcal{A}^*) - \chi_h^{\mathcal{A}^*}\|_{0,T} \leq \min(|T|^{1/2}, \gamma^{-1} h^{-t} \|y^* - i_h^y y_h^*\|_{0,T}),$$

which converges to zero whenever $\|y^* - i_h^y y_h^*\|_{0,T} = O(h^q), q > t$. Likewise, for $T \subset \mathcal{I}^*$ one can show that $\|\chi(\mathcal{A}^*) - \chi_h^{\mathcal{A}^*}\|_{0,T} \to 0$ as $h \to 0$. Now, for fixed $0 < \kappa \leq 1$ and $0 < t' \leq t$ (e.g., $\kappa = 0.5$ and $t' = t$), we provide approximations $\hat{\mathcal{A}}_h^*$ of $\mathcal{A}^*$ and $\hat{\mathcal{I}}_h^*$ of $\mathcal{I}^*$ according to

$$\hat{\mathcal{A}}_h^* := \bigcup \{T \in \mathcal{T}_h \mid \chi_h^{\mathcal{A}^*}(x) \geq 1 - \kappa h^{t'} \text{ for all } x \in T\}, \tag{3.16a}$$

$$\hat{\mathcal{I}}_h^* := \bigcup \{T \in \mathcal{T}_h \mid \chi_h^{\mathcal{A}^*}(x) < 1 - \kappa h^{t'} \text{ for some } x \in T\}. \tag{3.16b}$$

We define approximations $\mathcal{T}_{\mathcal{A}^* \cap \mathcal{A}_h^*}, \mathcal{T}_{\mathcal{I} \cap \mathcal{A}_h^*}$, and $\mathcal{T}_{\mathcal{A}^* \cap \mathcal{I}_h^*}$ of $\mathcal{A}^* \cap \mathcal{A}_h^*$, $\mathcal{I}^* \cap \mathcal{A}_h^*$, and $\mathcal{A}^* \cap \mathcal{I}_h^*$ by means of

$$\mathcal{T}_{\mathcal{A}^* \cap \mathcal{A}_h^*} := \hat{\mathcal{A}}_h^* \cap \mathcal{A}_h^*, \quad \mathcal{T}_{\mathcal{I}^* \cap \mathcal{A}_h^*} := \hat{\mathcal{I}}_h^* \cap \mathcal{A}_h^*, \quad \mathcal{T}_{\mathcal{A}^* \cap \mathcal{I}_h^*} := \hat{\mathcal{A}}_h^* \cap \mathcal{I}_h^*.$$

If $\operatorname{int}(\hat{\mathcal{I}}_h^*) \neq \emptyset$ and $\operatorname{int}(\hat{\mathcal{A}}_h^*) \neq \emptyset$, we introduce

$$\mu_{\hat{\mathcal{F}}_h^*} := - \frac{\partial p_h^*|_{\hat{\mathcal{I}}_h^*}}{\partial n_{\hat{\mathcal{I}}_h^*}} + \alpha \frac{\partial \Delta b}{\partial n_{\hat{\mathcal{A}}_h^*}} \tag{3.17}$$

as an approximation of (3.15b), where $\hat{\mathcal{F}}_h^* := \partial \hat{\mathcal{A}}_h^* \cap \hat{\mathcal{I}}_h^*$. Based on (3.14a)–(3.14c), (3.15a), (3.15b), and (3.17) we are able to evaluate ψ_h for the four sets $\mathcal{I}^* \cap \mathcal{I}_h^*$, $\mathcal{A}^* \cap \mathcal{A}_h^*$, $\mathcal{A}^* \cap \mathcal{I}_h^*$, $\mathcal{I}^* \cap \mathcal{A}_h^*$, which form a partitioning of Ω.

Case 1: $(\mathcal{I}^* \cap \mathcal{I}_h^*)$. Due to $\mu^* = 0$ on $\mathcal{I}^*$ and $\lambda_h^* = 0$ on $\mathcal{I}_h^*$, we obviously have

$$\psi_h|_{\mathcal{I}^* \cap \mathcal{I}_h^*} = \frac{1}{2} \left(\sum_{a \in \mathcal{N}_h(\mathcal{F}_h^* \cap \mathcal{I}^*)} \kappa_a^* (y_h^* - y^*)(a) + (\mu^*|_{\mathcal{F}^*}, y_h^* - b)_{0, \mathcal{F}^* \cap \mathcal{I}_h^*} \right). \tag{3.18}$$

Here and below we use $\lambda_h^* = \sum_{a \in \mathcal{N}_h(\Omega)} \kappa_a^* \delta_a$. Since y^* is unknown, we approximate $y^*(a)$ by $\hat{y}_\ell^*(a)$, where this approximation is obtained in the following way: We define

$$\mathcal{N}_h(a) := \{a\} \cup \{a' \in \mathcal{N}_h(\bar{\Omega}) \mid a' \text{ and } a \text{ are connected by an edge } e \in \mathcal{E}_h(\bar{\Omega})\}$$

and set

$$\hat{y}_\ell^*(a) := \operatorname{card}(\mathcal{N}_h(a))^{-1} \sum_{a' \in \mathcal{N}_h(a)} y_\ell^*(a').$$

This leads to the following approximations:

$$\hat{\psi}_h^{(1)} := \sum_{T\in\mathcal{T}_h} \hat{\psi}_T^{(1)}, \tag{3.19}$$

$$\hat{\psi}_T^{(1)} := \begin{cases} \frac{1}{4}\|\mu_{\hat{\mathcal{F}}_h^*}\|_E \|y_h^* - b\|_E, & T \in \{T_\pm\}, E = T_+ \cap T_- \in \mathcal{E}_h(\hat{\mathcal{F}}_h^*), \\ 0, & \text{otherwise}, \end{cases}$$

$$\hat{\psi}_h^{(2)} := \sum_{T\in\mathcal{T}_h} \hat{\psi}_T^{(2)}, \tag{3.20}$$

$$\hat{\psi}_T^{(2)} := \begin{cases} \frac{1}{2}\sum_{a\in\mathcal{N}_h(T)} |(y_h^* - \hat{y}_h^*)(a)|\kappa_a^*, & T \in \mathcal{T}_{\hat{\mathcal{F}}_h^*}, \\ 0, & \text{otherwise}, \end{cases}$$

and we thus arrive at the approximation

$$\hat{\psi}_h|_{\hat{\mathcal{I}}_h^*\cap\mathcal{I}_h^*} = \hat{\psi}_h^{(1)} + \hat{\psi}_h^{(2)}. \tag{3.21}$$

Here, we use $\mathcal{T}_{\hat{\mathcal{F}}_h^*} := \{T \in \mathcal{T}_h(\Omega) : \mathcal{E}_h(T) \cap \hat{\mathcal{F}}_h^* \neq 0\}$.

Case 2: $(\mathcal{A}^* \cap \mathcal{A}_h^*)$. In view of $y^* = b,\ y_h^* = b_h$ on $\mathcal{A}^* \cap \mathcal{A}_h^*$, and (3.14c), we obtain

$$\psi_h|_{\mathcal{A}^*\cap\mathcal{A}_h^*} = \frac{1}{2}\Big((z - b - \alpha\Delta^2 b, b_h - b)_{0,\mathcal{A}^*\cap\mathcal{A}_h^*} + (\mu_{\mathcal{F}^*}^*, b_h - b)_{0,\mathcal{F}^*\cap\mathcal{A}_h^*}\Big). \tag{3.22}$$

We introduce

$$\hat{\psi}^{(3)} := \sum_{T\in\mathcal{T}_h} \hat{\psi}_T^{(3)}, \tag{3.23}$$

$$\hat{\psi}_T^{(3)} := \begin{cases} \frac{1}{2}\|z - b - \alpha\Delta^2 b\|_T \|b - b_h\|_T, & T \in \mathcal{T}_{\hat{\mathcal{A}}_h^*\cap\mathcal{A}_h^*}, \\ 0, & \text{otherwise}, \end{cases}$$

and thus get the approximation

$$\hat{\psi}_h|_{\hat{\mathcal{A}}_h^*\cap\mathcal{A}_h^*} = \hat{\psi}_h^{(1)} + \hat{\psi}_h^{(3)}. \tag{3.24}$$

Case 3: $(\mathcal{A}^* \cap \mathcal{I}_h^*)$. Taking $y^* = b$ on $\mathcal{A}^*$ and $\lambda_h^* = 0$ on $\mathcal{I}_h^*$, as well as (3.14a)–(3.14b) into account, we get

$$\psi_h|_{\mathcal{A}^*\cap\mathcal{I}_h^*} = \frac{1}{2}\Big((\mu^*, y_h^* - b)_{0,\mathcal{A}^*\cap\mathcal{I}_h^*} + (\mu_{\mathcal{F}^*}^*, y_h^* - b)_{0,\mathcal{F}^*\cap\mathcal{I}_h^*}\Big). \tag{3.25}$$

Setting

$$\hat{\psi}_h^{(4)} := \sum_{T\in\mathcal{T}_h} \hat{\psi}_T^{(4)}, \tag{3.26}$$

$$\hat{\psi}_T^{(4)} := \begin{cases} \frac{1}{2}\|z - b - \alpha\Delta^2 b\|_T \|y_h^* - b\|_T, & T \in \mathcal{T}_{\hat{\mathcal{A}}_h^*\cap\mathcal{I}_h^*}, \\ 0, & \text{otherwise}, \end{cases}$$

it follows that an approximation is given by

$$\hat{\psi}_h|_{\hat{\mathcal{A}}_h^*\cap\mathcal{I}_h^*} = \hat{\psi}_h^{(1)} + \hat{\psi}_h^{(4)}. \tag{3.27}$$

Case 4: $(\mathcal{I}^* \cap \mathcal{A}_h^*)$. Finally, observing $\mu^* = 0$ on $\mathcal{I}^*$ and $y_h^* = b_h$ on $\mathcal{A}_h^*$ as well as (3.14a)–(3.14b), for the fourth set we have

$$\psi_h|_{\mathcal{I}^* \cap \mathcal{A}_h^*} = \frac{1}{2}\left(\sum_{a \in \mathcal{N}_h(\mathcal{I}^* \cap \mathcal{A}_h^*)} \kappa_a^* (y_h^* - y^*)(a) + (\mu_{\mathcal{F}^*}^*, b_h - b)_{0, \mathcal{F}^* \cap \mathcal{A}_h^*} \right). \tag{3.28}$$

Introducing

$$\begin{aligned} \hat{\psi}_h^{(5)} &:= \sum_{T \in \mathcal{T}_h} \hat{\psi}_T^{(5)}, \\ \hat{\psi}_T^{(5)} &:= \begin{cases} \frac{1}{2} \sum_{a \in \mathcal{N}_h(T)} |(y_h^* - \hat{y}_h^*)(a)| \kappa_a^*, & T \in \mathcal{T}_{\mathcal{I}_h^* \cap \mathcal{A}_h^*}, \\ 0, & \text{otherwise}, \end{cases} \end{aligned} \tag{3.29}$$

we obtain the approximation

$$\hat{\psi}_h|_{\hat{\mathcal{I}}_h^* \cap \mathcal{A}_h^*} = \hat{\psi}_h^{(1)} + \hat{\psi}_h^{(5)}. \tag{3.30}$$

3.2.2. Nonregular case. The nonregular case assumes the following structure of the active set $\mathcal{A}^*$:

(A_2) $\mathcal{A}^*$ is a Lipschitzian, strongly non–self-intersecting curve in Ω.

We note that a curve $\mathcal{C}$ is said to be strongly non–self-intersecting if, for every $a \in \mathrm{int}(\mathcal{C})$, there exists an open neighborhood $\mathcal{U}(a)$ such that $\mathcal{U}(a) \setminus \mathcal{C}$ consists of two connected components. Hence, $\mathcal{A}^*$ divides Ω into two connected components Ω_+ and Ω_-.

Again, since the Slater condition (1.1) implies $\mathcal{A}^* \cap \Gamma = \emptyset$, [6, Theorem 4] provides the following optimality characterization:

$$(\nabla p^*, \nabla w)_{0,\Omega} = (z - y^*, w) - \langle \lambda^*, w \rangle, \quad w \in W^{1,r}(\Omega), \tag{3.31a}$$

$$\lambda^* = \mu_{\mathcal{A}^*}^* = \nu_{\mathcal{A}^*} \cdot \nabla p^*|_{\mathcal{A}_+^*} - \nu_{\mathcal{A}^*} \cdot \nabla p^*|_{\mathcal{A}_-^*}, \tag{3.31b}$$

where $\nu_{\mathcal{A}^*}$ denotes the unit outer normal to $\mathcal{A}^*$ pointing towards $\mathcal{A}_+^* := \mathcal{A}^* \cap \bar{\Omega}_+$ and $\mathcal{A}_-^* := \mathcal{A}^* \cap \bar{\Omega}_-$.

We further define $\mu_{\hat{\mathcal{F}}_h^*}^*$ according to

$$\mu_{\hat{\mathcal{F}}_h^*}^* := \begin{cases} \nu_{\mathcal{A}_h^*} \cdot \nabla p_h^*|_{\mathcal{A}_h^*} - \nu_{\mathcal{I}_h^*} \cdot \nabla p_h^*|_{\mathcal{I}_h^*} & \text{if } \mathrm{meas}(\mathcal{A}_h^*) > 0, \\ \nu_{\mathcal{A}_h^*} \cdot \nabla p_h^*|_{\mathcal{A}_{h,+}^*} - \nu_{\mathcal{A}_h^*} \cdot \nabla p_h^*|_{\mathcal{A}_{h,-}^*} & \text{if } \mathrm{meas}(\mathcal{A}_h^*) = 0, \end{cases} \tag{3.32}$$

where, for $\mathrm{meas}(\mathcal{A}_h^*) = 0$, $\nu_{\mathcal{A}_h^*}$ and $\mathcal{A}_{h,\pm}^*$ are defined as in the continuous case.

As in the regular case, we evaluate ψ_h for the four sets $\mathcal{I}^* \cap \mathcal{I}_h^*$, $\mathcal{A}^* \cap \mathcal{A}_h^*$, $\mathcal{A}^* \cap \mathcal{I}_h^*$, $\mathcal{I}^* \cap \mathcal{A}_h^*$. We refer to $\hat{\psi}_h^{(1)}$, $\hat{\psi}_h^{(2)}$, and $\hat{\psi}_h^{(5)}$ as the error terms given by (3.19), (3.20), and (3.29) with $\mu_{\hat{\mathcal{F}}_h^*}^*$ in (3.19) replaced by (3.32).

Case 1: $(\mathcal{I}^* \cap \mathcal{I}_h^*)$. We have

$$\hat{\psi}_h|_{\mathcal{I}_h^* \cap \mathcal{I}_h^*} = \hat{\psi}_h^{(1)} + \hat{\psi}_h^{(2)}. \tag{3.33}$$

Case 2: $(\mathcal{A}^* \cap \mathcal{A}_h^*)$. We infer the approximation

$$\hat{\psi}_h|_{\hat{\mathcal{A}}_h^* \cap \mathcal{A}_h^*} = \hat{\psi}_h^{(1)}. \tag{3.34}$$

Case 3: $(\mathcal{A}^* \cap \mathcal{I}_h^*)$. As in the second case we obtain

$$\hat{\psi}_h|_{\hat{\mathcal{A}}_h^* \cap \mathcal{I}_h^*} = \hat{\psi}_h^{(1)}. \tag{3.35}$$

Case 4: $(\mathcal{I}^* \cap \mathcal{A}_h^*)$. We get the approximation

$$\hat{\psi}_h|_{\hat{\mathcal{I}}_h^* \cap \mathcal{A}_h^*} = \hat{\psi}_h^{(1)} + \hat{\psi}_h^{(5)}. \tag{3.36}$$

3.3. Primal-dual weighted data oscillations. The data oscillation term $\widehat{osc}_h^{(2)}$ as given by (2.23) can be estimated by means of

$$\begin{aligned} \widehat{osc}_h^{(2)} &= \sum_{T \in \mathcal{T}_h} \widehat{osc}_T^{(2)}, \\ \widehat{osc}_T^{(2)} &:= \|f - f_h\|_{0,T} \|p_h^* - \hat{p}_h^*\|_{0,T} + \|z - z_h\|_{0,T} \|y_h^* - \hat{y}_h^*\|_{0,T}, \end{aligned} \tag{3.37}$$

where $\hat{p}_h^*$ is defined in the same way as $\hat{y}_h^*$ before (cf. section 3.2.1, Case 1).

We thus obtain the following upper bound for the data oscillations:

$$\widehat{osc}_h := \widehat{osc}_h^{(1)} + \widehat{osc}_h^{(2)}. \tag{3.38}$$

4. The adaptive algorithm. The adaptive finite element algorithm based on the goal-oriented dual weighted residuals consists of successive loops of the cycle

$$\text{SOLVE} \quad \Longrightarrow \quad \text{ESTIMATE} \quad \Longrightarrow \quad \text{MARK} \quad \Longrightarrow \quad \text{REFINE}\,.$$

Here, SOLVE stands for the numerical solution of the discrete optimality system (2.5a)–(2.5d), which is taken care of by the primal-dual active set strategy from [5]. The subsequent step ESTIMATE requires the computation of the estimates for the weighted dual residuals, the primal-dual mismatch in complementarity, and the data oscillations as derived in the previous section 3. The third step, MARK, takes care of the selection of elements of the triangulation $\mathcal{T}_h$ for refinement based on the information provided by the weighted dual residuals and the upper bounds for the primal-dual mismatch in complementarity and the data oscillations. For this selection process, we use a bulk criterion, also known as Dörfler marking [9], which will be described here in the regular case (the modifications in the nonregular case are obvious). Referring to $\rho_T^{(i)}, \hat{\omega}_T^{(i)}, 1 \le i \le 2$, $\hat{\psi}_T^{(i)}, 1 \le i \le 5$, and $\widehat{osc}_T^{(i)}, 1 \le i \le 2$, as the residuals (3.2a)–(3.2b) and estimates as given by (3.7a)–(3.7b), (3.19), (3.20), (3.23), (3.26), (3.29), and (2.15), (3.37), we select a subset $\hat{\mathcal{T}}_h$ of elements such that for some universal constant $0 < \Theta < 1$ we have

$$\begin{aligned} &\Theta \sum_{T \in \mathcal{T}_h} \left(\sum_{i=1}^{2} \rho_T^{(i)} \hat{\omega}_T^{(i)} + \sum_{i=1}^{5} \hat{\psi}_T^{(i)} + \sum_{i=1}^{2} \widehat{osc}_T^{(i)} \right) \\ &\le \sum_{T \in \hat{\mathcal{T}}_h} \left(\sum_{i=1}^{2} \rho_T^{(i)} \hat{\omega}_T^{(i)} + \sum_{i=1}^{5} \hat{\psi}_T^{(i)} + \sum_{i=1}^{2} \widehat{osc}_T^{(i)} \right). \end{aligned} \tag{4.1}$$

The bulk criterion can be realized by a greedy algorithm [14]. The final step REFINE is devoted to the technical realization of the refinement process.

5. Numerical results. We present numerical results for three test examples to illustrate the performance of the adaptive algorithm described in section 4. The first two examples, taken from [18] and [21], respectively, represent problems where the coincidence set (Example 2) or the main part of the coincidence set (Example 1) consists of a simply connected subdomain. The third example, considered in [18, 20], features a degeneration of the nonregular case with the coincidence set consisting of a single point. A similar construction was studied in [4]. We note that Examples 1 and 3 involve a given shift (or desired) control u^d; i.e., the objective functional is of the form

$$J(y,u) = \frac{1}{2}\|y-z\|^2_{0,\Omega} + \frac{\alpha}{2}\|u-u^d\|^2_{0,\Omega}.$$

This generalization is easily accommodated by the theory, since the shift control can be formally absorbed by the right-hand side of the state equation.

Example 1. The data of the problem are as follows:

$$\Omega := (-2,2)^2, \quad z := y^*(r) + \Delta p^*(r) + \lambda^*(r), \quad u^d := u^*(r) + \alpha^{-1}\, p^*(r),$$
$$f := 0, \quad b := 0, \quad \alpha := 0.1, \quad \Gamma := \partial\Omega.$$

Here, $y^* = y^*(r)$, $u^* = u^*(r)$, $p^* = p^*(r)$, and $\lambda^* = \lambda^*(r)$, $r := (x_1^2 + x_2^2)^{1/2}$, $(x_1, x_2)^T \in \Omega$, are chosen according to

$$y^*(r) := -r^{\frac{4}{3}}\,\gamma_1(r), \quad u^*(r) := -\Delta\, y^*(r),$$
$$p^*(r) := \gamma_2(r)\,\left(r^4 - \frac{3}{2}r^3 + \frac{9}{16}r^2\right), \quad \lambda^*(r) := \begin{cases} 0, & r < 0.75, \\ 0.1, & \text{otherwise}, \end{cases}$$

where

$$\gamma_1 := \begin{cases} 1, & r < 0.25, \\ -192(r-0.25)^5 + 240(r-0.25)^4 - 80(r-0.25)^3 + 1, & 0.25 < r < 0.75, \\ 0, & \text{otherwise}, \end{cases}$$

$$\gamma_2 := \begin{cases} 1, & r < 0.75, \\ 0, & \text{otherwise}. \end{cases}$$

We note that the constraint b does not satisfy (1.1). However, it is easy to check that the above functions satisfy the optimality conditions (1.2a)–(1.2c).

The optimal state y^* strongly oscillates around the origin, with the coincidence set given by $\mathcal{A}^* = \{(r,\varphi) | 0.25 < r < 1\ ,\ 0 \le \varphi < 2\pi\} \cup \{(0,0)\}$ (cf. Figure 5.1(left)). Figure 5.1(right) displays the adaptively refined mesh after 26 refinement steps. As can be clearly seen, the free boundary $\mathcal{F}^*$ between the coincidence set and the non-coincidence set is well resolved.

The performance of the adaptive algorithm is illustrated in Figure 5.2(left), where the absolute error in the quantity of interest (objective functional) is shown on a logarithmic scale as a function of the total number of degrees of freedom (DoF), both for adaptive refinement ($\theta = 0.5$) and uniform refinement. Figure 5.2(right) reflects the convergence history in the asymptotic regime by displaying the refinement level ℓ, the corresponding DoF, and the values of the absolute error $|J^* - J_h^*| := |J(y^*,u^*) - J_h(y_h^*,u_h^*)|$ in the objective functional as well as the associated effectivity indices $\mathrm{Eff} := \eta_h / |J(y^*,u^*) - J_h(y_h^*,u_h^*)|$, where η_h comprises the approximations of the primal-dual residuals, the primal-dual mismatch in complementarity, and the data

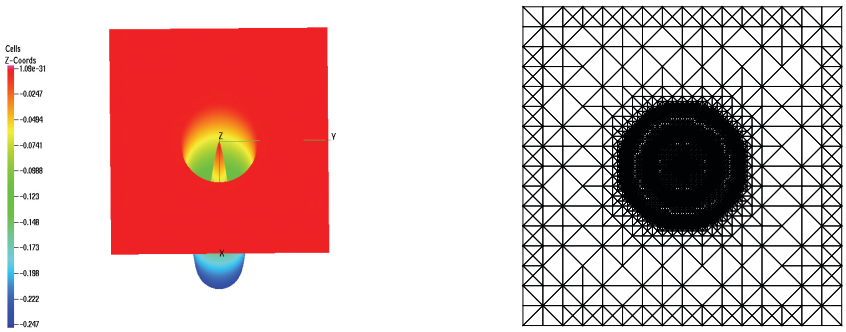

FIG. 5.1. *Example* 1: *Optimal state* y^* *(left) and refined mesh after* 26 *refinement steps (right).*

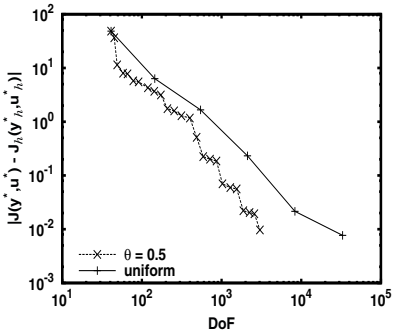

ℓ	DoF	$\lvert J^* - J^*_\ell \rvert$	Eff.Ind.
26	3030	9.69E-03	1.28
27	3618	7.86E-03	1.31
28	4255	7.07E-03	1.27
29	5042	6.78E-03	1.14
30	6048	5.56E-03	1.18
31	7177	5.17E-03	1.05

FIG. 5.2. *Example* 1: *Decrease of the error in the objective functional as a function of the DoF for adaptive refinement* ($\theta = 0.5$) *and uniform refinement on a logarithmic scale (left); convergence history of the adaptive refinement process including effectivity indices (right).*

oscillations. We observe that η_h provides an upper bound of the absolute error in the objective functional with effectivity indices being only slightly larger than 1.

Example 2. The data of the problem are as follows:

$$\Omega := (0,1)^2, \quad \Gamma = \partial\Omega, \quad z := 2x_1x_2,$$
$$u^d(r) := 0, \quad \alpha := 10^{-3}, \quad f := 0, \quad b := 0.55.$$

The upper bound b has been selected such that the coincidence set is a very small subset of Ω (cf. Figure 5.3(left)). However, an analytical representation is not known, either of the exact optimal solution or of the coincidence set. As a substitute for the exact solution we have chosen the computed solution with respect to a sufficiently fine simplicial triangulation of the computational domain.

The computed substitute for the exact optimal state y^* is shown in Figure 5.3(left) along with the associated coincidence set. Figure 5.3(right) displays the adaptively generated mesh after 17 refinement steps ($\theta = 0.5$), reflecting a pronounced refinement in and around the coincidence set. This is due to a singularity of the adjoint state in the active zone. Correspondingly, the estimator is dominated by the terms $\hat{\omega}_T^{(2)}\rho_T^{(2)}$ in the primal-dual weighted part (cf. (3.8)) and the terms $\hat{\psi}_T^{(1)}$ in the primal-dual mismatch in complementarity (cf. (3.19)), which explains the extensive refinement in and around the coincidence set.

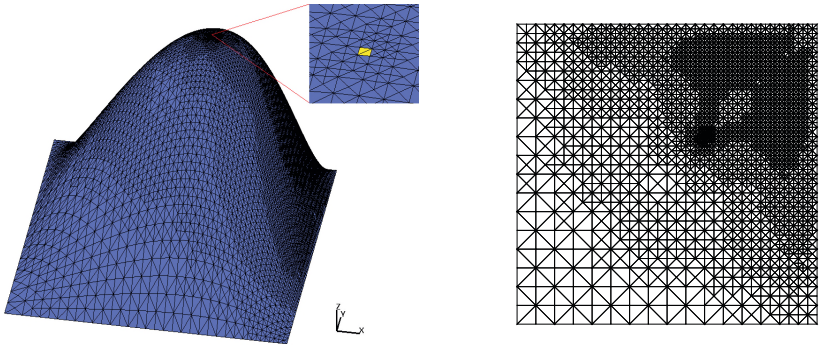

FIG. 5.3. *Example* 2: *Computed optimal state* y_h^* *(left) and refined mesh after* 17 *refinement steps (right).*

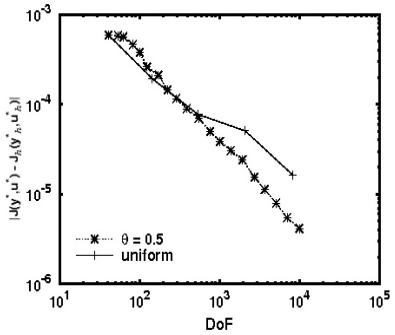

ℓ	DoF	$\lvert J^* - J_\ell^* \rvert$	Eff.Ind.
16	1951	2.41E-05	6.41
17	2748	1.55E-05	5.91
18	3691	1.13E-05	6.66
19	5119	7.96E-06	6.43
20	7066	5.46E-06	7.42
21	10040	4.15E-06	6.63

FIG. 5.4. *Example* 2: *Decrease of the error in the objective functional as a function of the DoF for adaptive refinement* ($\theta = 0.5$) *and uniform refinement on a logarithmic scale (left); convergence history of the adaptive refinement process including effectivity indices (right)).*

Figure 5.4(left) is devoted to a comparison of adaptive refinement ($\theta = 0.5$) and uniform refinement. The table in Figure 5.4(right) shows the asymptotic behavior in terms of the refinement level ℓ, the corresponding DoF, the values of the absolute error in the objective functional, and the associated effectivity indices.

Example 3. As stated in the introduction, our proof technique and the resulting error estimators are readily carried over to other types of boundary conditions. In this respect, we now consider a governing equation with homogeneous Neumann (rather than Dirichlet) boundary conditions. This problem was also used in a different context in [20], where the corresponding first order optimality conditions may be found, as well. In fact, we consider

$$-\Delta y + y = u + f \quad \text{in } \Omega, \qquad \frac{\partial y}{\partial n} = 0 \quad \text{on } \Gamma = \partial\Omega.$$

In our numerical tests we use

$$\Omega := B(0,1), \quad z := 4 + \frac{1}{\pi} - \frac{1}{4\pi} r^2 + \frac{1}{2\pi} \ln(r),$$
$$u^d(r) := 4 + \frac{1}{4\pi} r^2 - \frac{1}{2\pi} \ln(r), \quad \alpha := 1.0, \quad f := 0, \quad b(r) := r + 4.$$

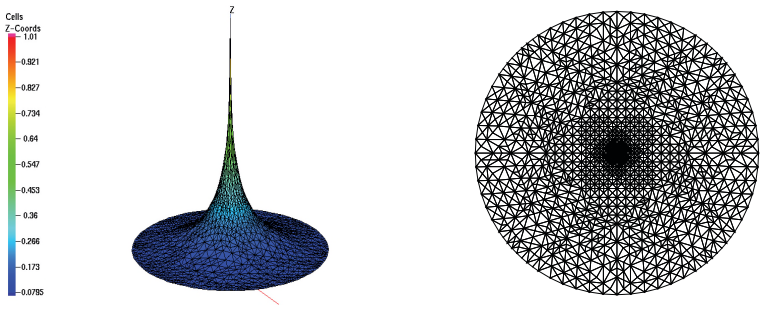

FIG. 5.5. *Example* 2: *Computed optimal adjoint state* p_h^* *(left) and refined mesh after* 20 *refinement steps (right).*

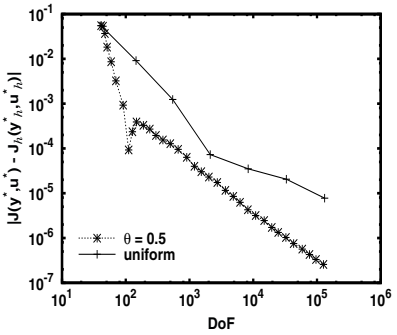

ℓ	DoF	$\lvert J^* - J_\ell^* \rvert$	Eff.Ind.
31	32475	1.03E-06	6.93
32	43005	7.54E-07	7.91
33	58605	5.69E-07	7.93
34	76142	4.31E-07	8.22
35	96300	3.33E-07	8.25
36	125943	2.59E-07	8.23

FIG. 5.6. *Example* 2: *Decrease of the error in the objective functional as a function of the DoF for adaptive refinement* ($\theta = 0.5$) *and uniform refinement on a logarithmic scale (left); convergence history of the adaptive refinement process including effectivity indices (right).*

The optimal solution is given by

$$y^*(r) = 4, \quad p^*(r) = \frac{1}{4\pi} r^2 - \frac{1}{2\pi} \ln(r), \quad u^*(r) = 4, \quad \lambda^* = \delta_0,$$

where δ_0 denotes the Dirac-δ concentrated at the origin.

The optimal adjoint state p^* belongs to $W^{1,s}(\Omega)$ for any $s < 2$ and has a singularity at the origin which represents the coincidence set $\mathcal{A}^*$. The computed approximation p_h^* is displayed in Figure 5.5(left). The adaptively generated mesh after 20 refinement steps ($\theta = 0.5$), shown in Figure 5.5(right), reflects the singular behavior of the adjoint state.

Figure 5.6(left) provides a comparison of the convergence history for adaptive refinement ($\theta = 0.5$) and uniform refinement, whereas Figure 5.6(right) contains the refinement level ℓ, the corresponding DoF, the values of the absolute error in the objective functional, and the associated effectivity indices in the asymptotic regime. The estimator provides an upper bound for the error, with the actual error being overestimated by a factor of approximately 8. At the initial stage of the refinement process, the estimator is dominated by the primal-dual mismatch in complementarity and the data oscillations, whereas in the asymptotic regime the terms $\hat{\omega}_T^{(2)} \rho_T^{(2)}$ in the primal-dual weighted residuals prevail due to the singularity of the adjoint state in the origin.

In all three examples, the true error is slightly overestimated, in contrast to [21, Example 2] and [4, Example 3], where an underestimation is reported. This is partly due to the incorporation of the primal-dual mismatch in complementarity. However, the amount of overestimation is less pronounced than for standard residual-type a posteriori error estimators (see [18, Examples 1 and 3]).

REFERENCES

[1] W. Bangerth and R. Rannacher, *Adaptive Finite Element Methods for Differential Equations*, Birkhäuser, Zürich, 2003.

[2] R. Becker and R. Rannacher, *An Optimal Control Approach to Error Estimation and Mesh Adaptation in Finite Element Methods*, Acta Numer. 10, Cambridge University Press, Cambridge, UK, 2001, pp. 1–102.

[3] R. Becker, H. Kapp, and R. Rannacher, *Adaptive finite element methods for optimal control of partial differential equations: Basic concept*, SIAM J. Control Optim., 39 (2000), pp. 113–132.

[4] O. Benedix and B. Vexler, *A posteriori error estimation and adaptivity for elliptic optimal control problems with state constraints*, Comput. Optim. Appl., 44 (2009), pp. 3–25.

[5] M. Bergounioux, M. Haddou, M. Hintermüller, and K. Kunisch, *A comparison of a Moreau–Yosida-based active set strategy and interior point methods for constrained optimal control problems*, SIAM J. Optim., 11 (2000), pp. 495–521.

[6] M. Bergounioux and K. Kunisch, *On the structure of Lagrange multipliers for state constrained optimal control problems*, Systems Control Lett., 48 (2003), pp. 169–176.

[7] E. Casas, *Boundary control of semilinear elliptic equations with pointwise state constraints*, SIAM J. Control Optim., 31 (1993), pp. 993–1006.

[8] K. Deckelnick and M. Hinze, *Convergence of a finite element approximation to a state-constrained elliptic control problem*, SIAM J. Numer. Anal., 45 (2007), pp. 1937–1953.

[9] W. Dörfler, *A convergent adaptive algorithm for Poisson's equation*, SIAM J. Numer. Anal., 33 (1996), pp. 1106–1124.

[10] K. Erikson, D. Estep, P. Hansbo, and C. Johnson, *Introduction to Adaptive Methods for Differential Equations*, Acta Numer., Cambridge University Press, Cambridge, UK, 1995, pp. 105–158.

[11] A. Günther and M. Hinze, *A posteriori error control of a state constrained elliptic control problem*, J. Numer. Math., 16 (2008), pp. 307–322.

[12] M. Hintermüller and R. H. W. Hoppe, *Goal-oriented adaptivity in control constrained optimal control of partial differential equations*, SIAM J. Control Optim., 47 (2008), pp. 1721–1743.

[13] M. Hintermüller and R. H. W. Hoppe, *Goal oriented mesh adaptivity for mixed control-state constrained elliptic optimal control problems*, in Proceedings of the International Conference on Scientific Computing in Simulation, Optimization and Control, Jyväskylä, Finland, 2007, W. Fitzgibbon, Y. A. Kuznetsov, P. Neittaanmäki, J. Périaux, and O. Pironneau, eds., Comput. Methods Appl. Sci. 15, Springer, New York, 2010, pp. 97–111.

[14] M. Hintermüller, R. H. W. Hoppe, Y. Iliash, and M. Kieweg, *An a posteriori error analysis of adaptive finite element methods for distributed elliptic control problems with control constraints*, ESAIM Control Optim. Calc. Var., 14 (2008), pp. 540–560.

[15] M. Hintermüller and K. Kunisch, *Feasible and noninterior path-following in constrained minimization with low multiplier regularity*, SIAM J. Control Optim., 45 (2006), pp. 1198–1221.

[16] M. Hintermüller and K. Kunisch, *Stationary optimal control problems with pointwise state constraints*, in Numerical PDE Constrained Optimization, M. Heinkenschloss, L. N. Vicente, and L. M. Fernandes, eds., Lect. Notes Comput. Sci. Eng. 73, Springer, Berlin, 2009.

[17] R. H. W. Hoppe and M. Kieweg, *Adaptive finite element methods for mixed control-state constrained optimal control problems for elliptic boundary value problems*, Comput. Optim. Appl., 46 (2010), pp. 511–533.

[18] R. H. W. Hoppe and M. Kieweg, *A posteriori error estimation of finite element approximations of pointwise state constraint distributed parameter problems*, J. Numer. Math., 17 (2009), pp. 219–244.

[19] R. Li, W. Liu, H. Ma, and T. Tang, *Adaptive finite element approximation for distributed elliptic optimal control problems*, SIAM J. Control Optim., 41 (2002), pp. 1321–1349.

[20] C. Meyer, U. Prüfert, and F. Tröltzsch, *On two numerical methods for state-constrained elliptic problems*, Optim. Methods Softw., 22 (2007), pp. 871–899.

[21] A. Schiela and A. Günther, *Interior Point Methods in Function Space for State Constraints—Inexact Newton and Adaptivity*, ZIB-Report 09-01, Konrad-Zuse-Zentrum für Informationstechnik, Berlin, 2009.

[22] L. R. Scott and S. Zhang, *Finite element interpolation of nonsmooth functions satisfying boundary conditions*, Math. Comp., 54 (1990), pp. 483–493.

[23] B. Vexler and W. Wollner, *Adaptive finite elements for elliptic optimization problems with control constraints*, SIAM J. Control Optim., 47 (2008), pp. 509–534.

[24] W. Wollner, *A posteriori error estimates for a finite element discretization of interior point methods for an elliptic optimization problem with state constraints*, Comput. Optim. Appl., 47 (2010), pp. 133–159.